

Orientation analysis for rotated human face detection

Jie Zhou^a, Xiao guang Lu^a, David Zhang^{b,*}, Chen-yu Wu^a

^aDepartment of Automation, Tsinghua University, Beijing 100084, People's Republic of China

^bDepartment of Computing, Biometrics Technology Centre, The Hong Kong Polytechnic University, Hung Hum Kowloon, Hong Kong, People's Republic of China

Received 3 December 2000; received in revised form 21 November 2001; accepted 12 January 2002

Abstract

In this paper, we present a framework of orientation analysis for rotated human face detection. A novel orientation histogram is constructed for statistical analysis of face images, which can show a proper symmetry with respect to the orientation of the principal axis and a local peak at its orthogonal orientation. By analyzing the orientation histogram, we can easily find the principal axis' orientation of the rotated face. Then an upright frontal face detector based on orientation analysis and other knowledge is designed to verify the given face. The experimental results illustrate the effectiveness of our framework. © 2002 Elsevier Science B.V. All rights reserved.

Keywords: Pattern recognition; Orientation analysis; Human face detection; Orientation histogram

1. Introduction

Human face detection is important in a face recognition system, also quite useful in multimedia retrieval [1]. Many algorithms have been proposed for upright frontal face detection such as correlation templates [2], mosaic technique [3], deformable template matching [4], eigenface [5], and neural network [6,7] but they cannot work well when the face is rotated. Since users usually expect faces to be detected at any angle, it is necessary to develop an effective algorithm for rotated face detection. In this paper, we will mainly address the issue of detecting rotated face within the image plane, i.e. frontal face with any angle.

One can directly rotate an upright frontal face detector repeatedly by small increments to verify the existence of the face rotated within the image plane. Usually an upright face detector is invariant to 10° of rotation from upright (both clockwise and counterclockwise) and the entire detection procedure needs to be applied at least 18 times (20° per step) to each image. So, this is a computationally expensive task. Furthermore, it will also result in too many false alarms. The better way is first detecting the rotation angle and then applying the upright face detector only once. In Ref. [8], a neural network was proposed to detect the rota-

tion angle of the face image but the detection result is far from satisfaction (the correct ratio is only 92% when the error is limited with $\pm 10^\circ$).

Orientation is one of the basic characteristics in image understanding and pattern analysis. Since human face is a typical oriented pattern, it is natural to apply orientation analysis to detect the rotation angle of the given human face. Moreover, analyzing the supposed face's orientation can help one to verify its existence.

In this paper, we will develop a novel image histogram called *orientation histogram* for orientation analysis. As a typical case, we utilize it to human face detection rotated within the image plane. The orientation histogram of human face shows the symmetry with respect to the principal axis as well as a local peak occurs at its orthogonal angle. Then, we can determine the principal axis' orientation of the rotated face by analyzing the orientation histogram and develop a novel upright face detector based on both orientation analysis and other knowledge. As a result, the above schemes can be combined to detect human face rotated within the image plane.

The organization of this paper is arranged as follows: orientation histogram is proposed in Section 2. Section 3 analyzes the orientation characteristics in the human face and presents a detection algorithm for rotated human face. The experimental results and some conclusions are given in Sections 4 and 5, respectively.

* Corresponding author. Tel.: +86-852-2766-7271; fax: +86-852-2774-0842.

E-mail address: csdzhang@comp.polyu.edu.hk (D. Zhang).

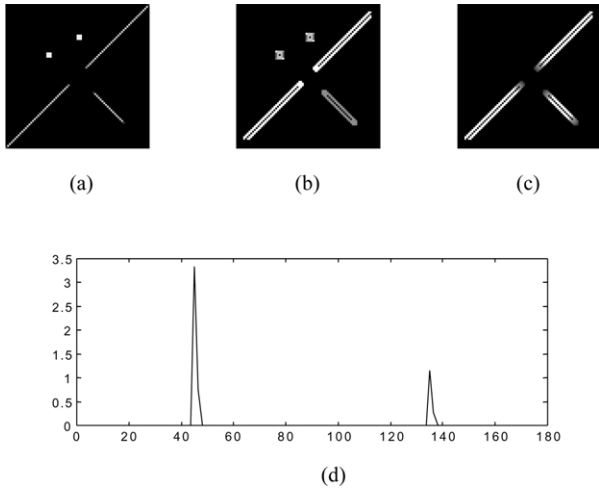


Fig. 1. Illustrations of orientation analysis: (a) original image; (b) orientation map (on a gray scale from 180°, white to 0°, gray; the pixels in black are not considered); (c) anisotropic strength map on a gray scale from 0, black to 1, white; (d) orientation histogram.

2. Orientation histogram

In this section, we first introduce a conventional orientation analysis method, i.e. *local orientation analysis*.

Then, a new image histogram, *orientation histogram*, is defined for orientation analysis.

2.1. Local orientation analysis

As an important orientation analysis method designed for singular point detection, the method was firstly proposed by Kass and Witkin [9] and further developed by Yang et al. [10,11].

It has been demonstrated that for a strongly oriented intensity pattern along one direction the power spectrum of such a pattern clusters along a line through the origin in Fourier transformation domain and the direction of the line is perpendicular to the dominant spatial orientation. Instead of the actual computation in the Fourier transformation domain the orientation map, $\theta(x, y)$, and anisotropic strength map, $g(x, y)$, can be calculated directly from intensity image, $I(x, y)$, and its first order partial derivatives by

$$\theta(x, y) = \frac{1}{2} \tan^{-1} \frac{\iint_{\Omega} 2I_x I_y dx dy}{\iint_{\Omega} (I_x^2 - I_y^2) dx dy} + \frac{\pi}{2}, \quad (1)$$

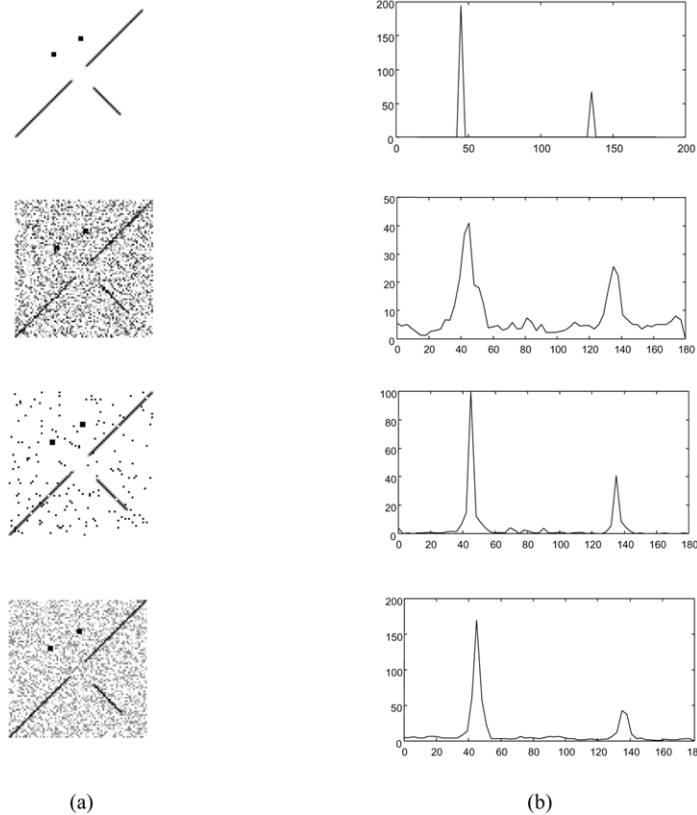


Fig. 2. The orientation histograms of noised images: (a) images by adding original image with no noise, Gaussian noise, black–white noise and speckle noise from top to bottom and (b) the corresponding orientation histograms.

$$g(x, y) = \frac{\left(\iint_{\Omega} (I_x^2 - I_y^2) dx dy\right)^2 + \left(\iint_{\Omega} 2I_x I_y dx dy\right)^2}{\left(\iint_{\Omega} (I_x^2 + I_y^2) dx dy\right)^2}, \quad (2)$$

where \tan^{-1} is a four-quadrant arctangent function, I_x and I_y are partial derivatives of $I(x, y)$, respectively. Note that Ω is a small neighborhood of pixel, (x, y) , whose size is related with the size of the object that we want to analyze. The value of anisotropic strength, g , is between 0 and 1 (close to 1 for a strongly oriented pattern, and 0 for isotropic regions).

Local orientation analysis can give the measure of orientation's strength in Eq. (2) besides the distribution of orientation (using Eq. (1)), which is different from other conventional orientation analysis tools, such as Gabor Transform [12]. Due to the use of first-order derivatives in Eqs. (1) and (2) the measure of orientation and its strength is insensitive to the irregular illumination of the images. Due to the integration in Eqs. (1) and (2) the measure can also be relatively insensitive to noise.

It should be addressed that the orientation mentioned earlier refers to collinear orientation, i.e. if two orientations are collinear (i.e. the difference between them is π), they should be considered as the same orientation so that the domain of θ is $[0, \pi]$.

2.2. Orientation histogram design

In order to analyze the distribution of orientations statistically, we develop a new histogram, orientation histogram, by combining the orientation's distribution and its strength

$$H(\alpha) = \sum_{\theta(x,y)=\alpha} g(x, y), \quad (3)$$

where α is the angle of any orientation between 0 and π , and $g(x, y)$ is the anisotropic strength of pixel, (x, y) , whose orientation, $\theta(x, y)$, is α . For one image, Eq. (3) represents the sum of anisotropic strength along the orientation, α . It is clear that $H(\alpha)$ is a π -periodic function.

This orientation histogram defined can be used for statistical analysis of the images. Since local orientation analysis is insensitive to both irregular lightening and noise, orientation histogram also has such ability. As an example shown in Fig. 1, there are two strong oriented patterns along the angles of $\pi/4$ and $3\pi/4$, so the orientation histogram has two peaks at $\pi/4$ and $3\pi/4$, respectively. Note that the anisotropic strengths of their point patterns are 0, which means the spurious orientation generated by such noises can be restrained. A further illustration is shown in Fig. 2, in which the original image is added with different types of random noise: Gaussian noise, black–white noise and speckle noise. However, their orientation histograms are rather robust. It shows that the orientation histogram has a good ability of noise resistance.

Theoretically, the rotation within image plane causes the translation of the periodic histogram, $H(\alpha)$. After the digitization, this relationship is still approximately held.

Orientation histogram can also be used for other applications. For example, we have applied to automatic cartridge identification and the results are rather satisfying. Readers can see Ref. [13] for details.

3. Orientation based face detection

Face detection is to distinguish human face from other patterns. Here, we consider the face images in a novel perspective—orientation.

3.1. Oriented patterns in human face

In the human faces, each organ has its own orientation in $[0, 2\pi)$. If the face is upright and frontal the orientations of organs can be roughly divided into two groups: horizontal (for most organs such as eyebrows, mouth and eyes) and vertical (for nose and cheek). Also human face has strong symmetry along the nose vertically. We define this symmetry axis as a *principal axis* and the organs such as eyebrow, mouth and eye are reflectionally symmetric (i.e. mirror symmetric) with respect to its principal axis (note that reflectional symmetry is different from centric symmetry as described in Refs. [14,15]). This symmetry is invariant to rotation within the image plane.

Let β be the orientation of the principal axis and $\theta(p)$ denote the orientation of one pixel, p . Also, we define \hat{p} as the pixel symmetric to p with respect to the principal axis. As mentioned earlier, a typical human face rotated within the image plane should satisfy

$$\theta(p) = 2\beta - \theta(\hat{p}). \quad (4)$$

From Eq. (3), it can be easily proved that its orientation histogram, $H(\alpha)$, should be reflectional symmetric with respect to β and $\beta + \pi/2$, i.e.

$$H(\alpha) = H(2\gamma - \alpha), \quad \gamma = \beta \text{ or } \beta + \pi/2, \quad (5)$$

where $\alpha \in [0, 2\pi)$.

The orientation histogram, $H(\alpha)$, of one face image cannot be strictly reflectional symmetric, hence we define a symmetry measure (SM) to reflect the degree of reflectional symmetry:

$$SM(\alpha) = \int_0^\pi |H(x) - H(2\alpha - x)| dx. \quad (6)$$

The smaller value of $SM(\alpha)$ shows a stronger reflectional symmetry with respect to α . When $H(\alpha)$ is strictly reflectional symmetric, $SM(\alpha)$ will be 0. Note that the cheek cannot influence the symmetry of the orientation histogram because that the cheek's orientation is nearly coincident to α .

Furthermore, a local peak will occur at the orientation

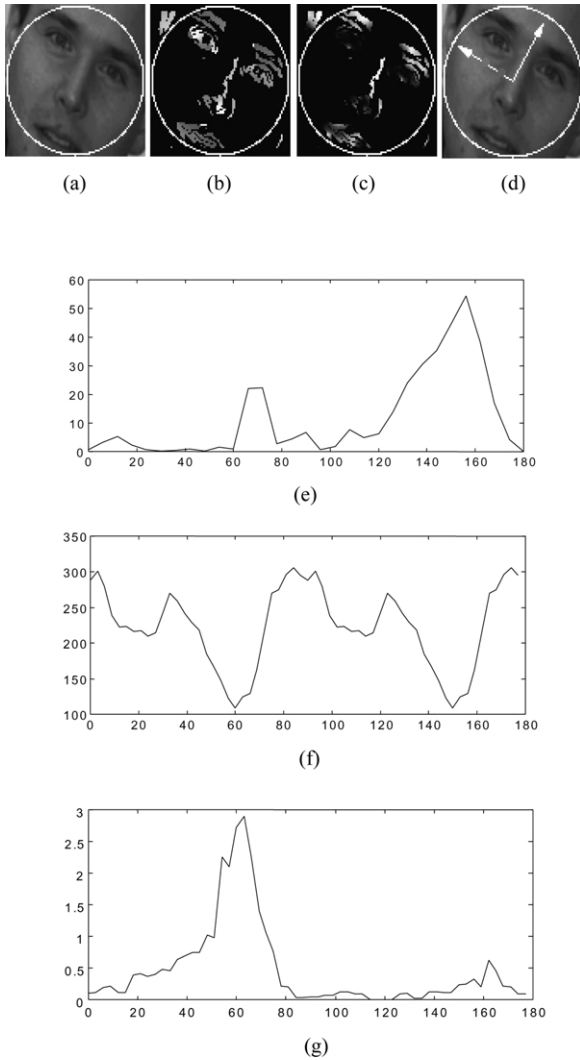


Fig. 3. Illustrations of finding the orientation of the principal axis: (a) original face image; (b) orientation map on a gray scale from 180° , white to 0° , gray; (c) anisotropic strength map from 0, black to 1, white; (d) the orientation of the principal axis, which is pointed by the solid arrow; (e) the orientation histogram; (f) symmetry measure; (g) OA measure. The orientation of principal axis is determined by the maximum of OA measure.

orthogonal to the principal axis since most organs in human face have strong oriented pattern at this orientation.

3.2. Extracting orientation from principal axis

For a rotated face within the image plane the orientation of the principal axis represents the face rotation status with respect to upright situation. Suppose that the input window contains one face, we can take the following steps to extract this orientation:

3.2.1. Calculate orientation histogram

For each pixel in the input window the orientation, θ , and anisotropic strength, g , are calculated, respectively. In order to remove the influence of orientation brought by small gray-level difference between pixels (for example, in

some smooth area, due to the quantization of gray-level the pseudo orientation may occur), we only consider the pixels whose gradient magnitude exceeds a threshold.

In a circular window mask the orientation histogram can be generated. The reason we use the circular window mask is to satisfy the isotropic computation. The orientation histogram can be obtained by

$$\hat{H}(\alpha) = \sum_{\theta(x,y) \in [\alpha - \text{bin}/2, \alpha + \text{bin}/2]} g(x,y), \quad \alpha = 0, \text{bin}, \text{bin} \times 2, \dots, \pi - \text{bin}, \quad (7)$$

where bin is the interval of two neighboring sampling orientation. Note that the resolution of orientation can be adjusted by bin.

3.2.2. Measure symmetry of orientation histogram

For any angle, α , we can measure the symmetry of the orientation histogram with respect to it by

$$\text{SM}(\alpha) = \sum_{\theta=0}^{\pi - \text{bin}} |\hat{H}(\theta) - \hat{H}(2\alpha - \theta)|, \quad \alpha = 0, \text{bin}, \text{bin} \times 2, \dots, \pi - \text{bin}. \quad (8)$$

3.2.3. Determine orientation of principal axis

$\hat{H}(\alpha)$ is symmetric with respect to β the orientation of the principal axis, so the symmetry measurement, $\text{SM}(\alpha)$, on this orientation results in a small value, maybe the minimum one.

Since orientations of the pixels in the oriented organs such as eyebrows and mouth are close to the orientation orthogonal to the principal axis, a local peak is generated at this orientation in the histogram, $\hat{H}(\alpha)$.

These two measurements, symmetry (nature in face) and peak (distribution of oriented pattern in face) can be combined together. Using both SM and local peak information, a criterion for determining the orientation of the principal axis can be created as follows:

$$\text{OA}(\alpha) = \frac{w_1 + w_2 h(\alpha + \pi/2)}{1 + w_3 \text{sm}(\alpha)}, \quad (9)$$

where $h(\alpha)$ and $\text{sm}(\alpha)$, which range from 0 to 1 denote the normalized $\hat{H}(\alpha)$ and $\text{SM}(\alpha)$, respectively; w_1 , w_2 and w_3 are three weighting factors that control the relative importance of both $h(\alpha)$ and $\text{sm}(\alpha)$.

Then, the orientation of the principal axis, α , can be obtained at which the maximum value of $\text{OA}(\alpha)$ is acquired. Fig. 3 gives an illustration on finding the orientation of the principal axis, where the dashed arrow points to the orientation at which the orientation histogram reaches the maximum value. The solid arrow points to the orientation of the principal axis, which is orthogonal to the orientation denoted by the dashed arrow. If a pixel's gradient magnitude is smaller than a given threshold, its orientation is not under consideration and its anisotropic strength is set to 0.

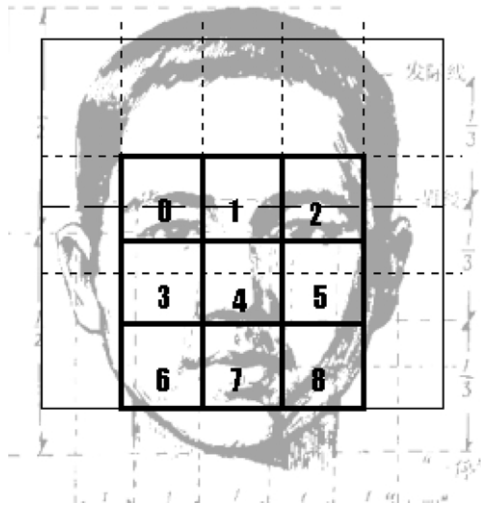


Fig. 4. The partition of upright human face for orientation analysis.

As mentioned in Section 3.1 the orientation of the principal axis can also be successfully detected even when some cheek is contained in the circular window. This means that our algorithm has a good robustness to the window's shift.

3.3. Upright face detector based on orientation analysis

The issue of upright face detection has been extensively addressed during the past decade. Among them, Yang and Huang's algorithm has been proved as a simple but effective way even robust under low-resolution condition [3]. The principal process is to divide the given image into several blocks and apply some knowledge based on the gray level and edges of main organs to test the existence of human face. This algorithm has a strong ability to detect human face, but at the same time it may result in rather high false alarm ratio.

As mentioned earlier the orientation is also one important characteristic of each face's organ, so we can combine it with other knowledge to develop a novel algorithm for upright face detection.

In order to describe the orientation of main organs, we separate an upright human face into 3×3 blocks as shown in Fig. 4, where Block 0 and Block 2 correspond to the regions of left eye (containing left eyebrow) and right eye (containing right eyebrow), respectively. Nose and mouth are corresponding to Block 4 and Block 7. In addition, both Blocks 3 and 5 are mainly the smooth area of the face. The orientation histogram of each block should satisfy:



Fig. 5. Some experimental results of the rotated face detection (the white circle is the circle mask used in calculating the histogram and the arrow refers to the orientation of the principal axis obtained by our algorithm).

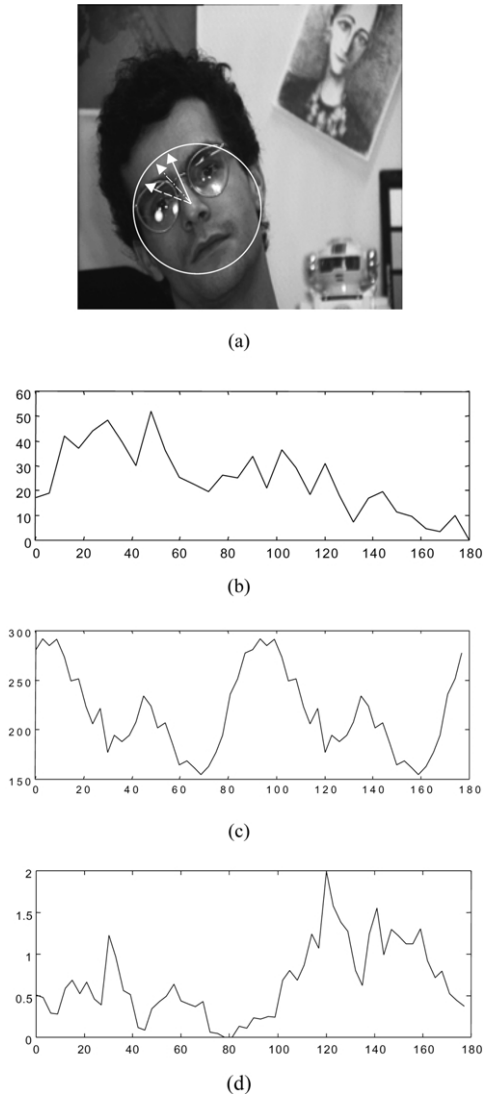


Fig. 6. The example to demonstrate the use of combining peak measure and SM: (a) original image, in which the white circles represent the detected area of face and the arrows with solid line, dashed line and split line denote the orientation of the principal axis detected by using the combination, peak criteria and symmetry criteria, respectively; (b) orientation histogram; (c) symmetry measure; (d) OA measure of the combination.

1. Blocks 0, 2 and 7: the orientation of eyes, eyebrows and mouth is mainly horizontal with rather strong orientation strength, so the orientation histogram will have a relative high peak at the angle corresponding to the horizontal;
2. Block 4: nose's orientation is mainly vertical and its orientation strength is not too strong, hence the orientation histogram will have a peak at the angle corresponding to the vertical, but the height of the peak is lower than block 0, 2 and 7;
3. Blocks 3 and 5: the orientation strength is rather weak.

These criteria considering orientation can be combined with the criterion proposed by Yang and Huang to verify the existence of upright human face.

In order to meet the need of rotated human face detection,

we can produce many detectors by rotating the template of the original upright face detector with different angles.

3.4. Detecting face rotated within the image plane

Now, we can combine the results stated earlier to construct a much faster framework for detecting rotated face within the image plane: using the algorithm described in Section 3.2 the orientation of the face's symmetry axis, i.e. rotation angle of supposed face image can be found. Then, we choose the face detector corresponding to that angle (which is produced from the original upright face detector as mentioned in Section 3.3) and apply it to verify the existence of the human face.

Because only one face detector is utilized for each window, the cost of computation for this framework is much smaller than applying upright face detector rotated step by step (at least 18 face detectors need to be used when the step interval is defined as 20°). The comparison of computing cost will be reported in Section 4.

4. Experimental results

Several experiments have been finished to verify the ability of the above framework. The algorithm is implemented in C language and based on a Pentium III 633 PC. The test set includes the face libraries from both MIT and our lab, all of which are real-life face images captured by CCD camera mainly in laboratory. They include faces in different situations, such as various lightening conditions as well as with beard or glasses. In our experiments, the bin of the histogram, $\hat{H}(\alpha)$, is set to 6° . The weighting factors in Eq. (9), w_1 , w_2 and w_3 are set to 0, 3 and 3, respectively. To detect faces anywhere in the image, our algorithm is applied to each location in the image. Circular windows' size is adjusted to accommodate the detection of faces with different sizes.

More than 150 face images rotated within the image plane, which cannot be directly extracted by conventional upright face detection systems along with more than 40 upright face images are tested. Our results are rather satisfying and the exact orientation of the principal axis can be detected for over 98% of the images (where the limit of detection error is set to $\pm 5^\circ$). This means that the orientation of their principal axis cannot be wrongly detected for most of the face images. Some of results are illustrated in Fig. 5.

The detector combining both peak measure and symmetry measure outperforms that using either one alone. The detection ratio of the principal axis' orientation is 98, 93 and 91% by using the combination, peak criteria and symmetry criteria, respectively. An example is given in Fig. 6. For the given face image the orientation detected by using peak measure or SM cannot conform to the real orientation of the principal axis but the decision by combining both criteria is correct.

For experimental images with noise and irregular lightening, our algorithm can work well for the detection of their

Table 1

The comparative results between our algorithm and the algorithm using the upright face detectors rotated step by step (20° each step)

	Upright face detector on the image rotated step by step	Our algorithm
Missing ratio (%)	9.8	10.3
False alarms #	120	45

principal axis' orientation. In our tests, there are also some face images rotated, a small angle ($<30^\circ$) out of the image plane (see the third row in Fig. 5). For these images, our algorithm can also successfully detect its orientation of principal axis.

One experiment is carried to compare our algorithm with the algorithm using the same upright face detector rotated step by step (20° each step). The result is listed in Table 1. The missing ratio of our algorithm has a slight increase from 9.8 to 10.3%, but the false alarm can have a sharp decrease from 120 to 45. The reason for the false alarms' reduction is that only one detector corresponding to a specific angle is utilized for each window and the false alarms caused by detectors corresponding to other angles can be avoided.

In our test, the average computing time of upright human

face detection is 0.072 s for an 80×80 window. On the other hand the computational cost of orientation analysis is 0.062 s for a window with the same size. If the window is slid to detect faces everywhere in a 256×240 image, 43 and 324 s are needed by using our algorithm and applying upright face detector rotated step by step (whose step interval is 20°), respectively. That is to say, more than 80% of the computational cost can be reduced by using our algorithm.

Another experiment is performed to test our algorithm proposed in Section 3.3 for detecting upright human face. Several photographs with complex background and multiple person are given to compare our algorithm and Yang and Huang's algorithm. There are totally 90 persons in these photographs. Some detection results are shown in Fig. 7 as well as a statistical result is listed in Table 2. The missing ratios of Yang and Huang's algorithm and our algorithm are 17.8 and 20.0%, respectively. The number of false alarms is 24 for Yang and Huang's algorithm but that of our algorithm is only 7. From them, we can see that much lower ratio of false alarm can be obtained while still maintaining a high ratio of right detection by using our algorithm.

5. Conclusions

In this paper, we develop a new orientation histogram



Fig. 7. Comparison between Yang and Huang's algorithm and our algorithm for detecting upright human face, where the top row is the result using Yang and Huang's algorithm; the bottom row is the result using our algorithm.

Table 2

The statistical results between Yang and Huang's algorithm and our algorithm for detecting the upright human face

	Yang and Huang's algorithm	Our algorithm
Missing ratio (%)	17.8	20.0
False alarms #	24	7

with a good ability to resist irregular lightening and noise, which can be applied to image's orientation analysis. Considering human face as an oriented and symmetric pattern, we analyze the obtained histogram in a given face window to detect the orientation of the principal axis in the face. It shows that the orientation of the principal axis can be exactly detected up to 98% of the images. We also propose a novel algorithm for the upright face detection systems, which is more effective than the conventional method by combining orientation with other knowledge. The experiments illustrate that more than 70% false alarms can be avoided while a high ratio of correct detection preserved. As a result, human face rotated within the image plane will be effectively detected by combining the algorithms of orientation detection of the principal axis and upright face detection, which is insensitive to lightening and viewpoint. Compared with the upright face detector rotated step by step, more than 80% of the computational cost can be reduced.

Acknowledgements

The authors wish to acknowledge support from Natural Science Foundation of China under grant 69775009. Also, the work is partially supported by the Centre for Multimedia Signal Processing in Hong Kong Polytechnic University.

References

- [1] R. Chellappa, C.L. Wilson, S. Sirohey, Human and machine recognition of faces: a survey, *Proc. IEEE* 83 (5) (1995) 705–740.
- [2] R. Brunelli, T. Poggio, Face recognition: features versus templates, *IEEE Trans. Pattern Anal. Mach. Intell.* 15 (10) (1993) 1042–1052.
- [3] G. Yang, T.S. Huang, Human face detection in a complex background, *Pattern Recogn.* 27 (1) (1994) 53–63.
- [4] A.L. Yuille, D.S. Cohen, P.W. Hallinan, Deformable templates for face recognition, *J. Cogn. Neurosci.* 3 (1989) 59–70.
- [5] M.A. Turk, A.P. Pentland, Face recognition using eigenfaces, *Proceedings of IEEE Computer Society Conference on Computer Vision and Pattern Recognition*, 1991, pp. 586–591.
- [6] S. Lin, S. Kung, L. Lin, Face recognition/detection by probabilistic decision-based neural network, *IEEE Trans. Neural Networks* 8 (1) (1997) 114–132.
- [7] H.A. Rowley, S. Baluja, T. Kanade, Neural network-based face detection, *IEEE Trans. Pattern Anal. Mach. Intell.* 20 (1) (1998) 23–38.
- [8] H.A. Rowley, S. Baluja, T. Kanade, Rotation invariant neural network-based face detection, *Proceedings of IEEE Computer Society Conference on Computer Vision and Pattern Recognition*, 1998, pp. 38–44.
- [9] M. Kass, A. Witkin, Analyzing oriented patterns, *Comput. Vision, Graph Image Process.* 37 (1987) 362–385.
- [10] G.Z. Yang, P. Burger, D.N. Firmin, S.R. Underwood, Structure adaptive anisotropic image filtering, *Image Vision Comput.* 14 (1996) 135–145.
- [11] F. Chabat, G.Z. Yang, D.M. Hansell, A corner orientation detector, *Image Vision Comput.* 17 (1999) 761–769.
- [12] J.G. Daugman, Uncertainty relation for resolution in space, spatial frequency, and orientation optimized by two-dimensional visual cortical filters, *J. Opt. Soc. Am.: A* 2 (1985) 1160–1169.
- [13] J. Zhou, L.P. Xin, G. Rong, D. Zhang, Algorithm of automatic cartridge identification, *Optical Engineering*, 40 (2001) 2860–2865.
- [14] D. Reissfeld, H. Wolfson, Y. Yeshurun, Detection of interest points using symmetry, *Proceedings of the Third International Conference on Computer Vision*, 1990, pp. 62–65.
- [15] D. Reissfeld, Y. Yeshurun, Robust detection of facial features by generalized symmetry, *Proceedings of the Eleventh International Conference on Pattern Recognition*, 1992, pp. 117–120.